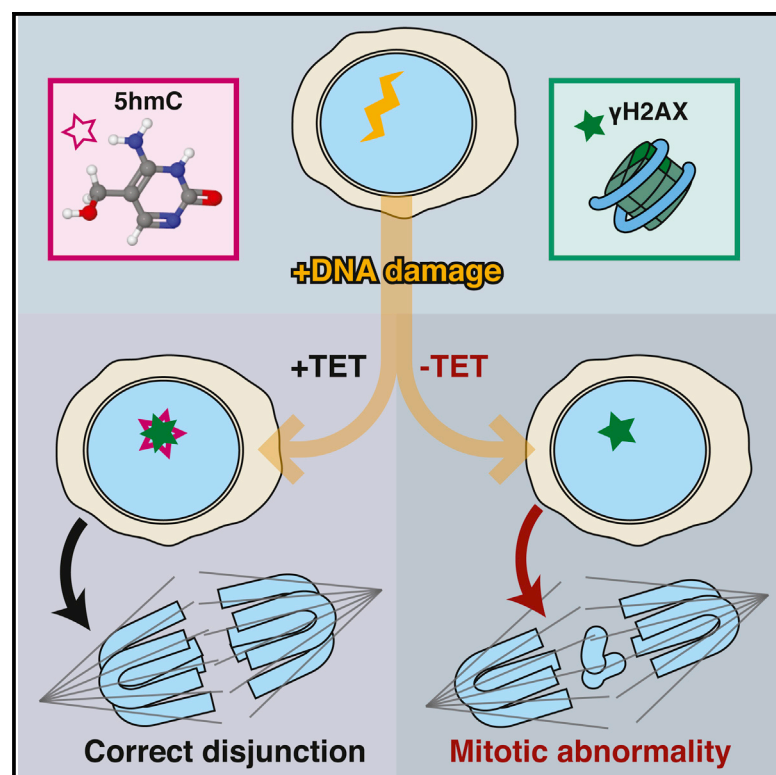# Cell Reports

5-Hydroxymethylcytosine Marks Sites of DNA Damage and Promotes Genome Stability

Graphical Abstract

Authors

Georgia Rose Kafer, Xuan Li, Takuro Horii, Isao Suetake, Shoji Tajima, Izuho Hatada, Peter Mark Carlton

Correspondence

pcarlton@icems.kyoto-u.ac.jp

In Brief

Kafer et al. demonstrate that DNA damage causes the modified DNA base 5-hydroxymethylcytosine (5hmC) to become locally enriched over broad chromosomal domains and that the TET enzymes promote correct chromosome segregation during replication stress.

Highlights

- 5hmC is actively enriched at endogenous DNA damage sites in cancer cell lines

- DNA damage induced by aphidicolin or microirradiation increases 5hmC locally

- TET2 is required to create damage-associated 5hmC foci in HeLa cells

- TET enzymes promote genome integrity under replication stress in mouse ES cells

Accession Numbers

GSE72998

CrossMark

CellPress

5-Hydroxymethylcytosine Marks Sites
of DNA Damage and Promotes Genome Stability

Georgia Rose Kafer,[1,4] Xuan Li,[1] Takuro Horii,[2] Isao Suetake,[3,4] Shoji Tajima,[3] Izuho Hatada,[2] and Peter Mark Carlton[1,4,5,*]
[1]Institute for Integrated Cell-Material Sciences (iCeMS), Kyoto University, Kyoto 606-8501, Japan
[2]Laboratory of Genome Science, Biosignal Genome Resource Center, Institute for Molecular and Cellular Regulation, Gunma University, Maebashi, Gunma 371-8511, Japan
[3]Laboratory of Epigenetics, Institute for Protein Research, Osaka University, Suita, Osaka 565-0871, Japan
[4]CREST, Japan Science and Technology Agency
[5]Present address: Graduate School of Biostudies, Kyoto University, Kyoto 606-8501, Japan
*Correspondence: pcarlton@icems.kyoto-u.ac.jp
http://dx.doi.org/10.1016/j.celrep.2016.01.035

SUMMARY

5-hydroxymethylcytosine (5hmC) is a DNA base created during active DNA demethylation by the recently discovered TET enzymes. 5hmC has essential roles in gene expression and differentiation. Here, we demonstrate that 5hmC also localizes to sites of DNA damage and repair. 5hmC accumulates at damage foci induced by aphidicolin and microirradiation and colocalizes with major DNA damage response proteins 53BP1 and γH2AX, revealing 5hmC as an epigenetic marker of DNA damage. Deficiency for the TET enzymes eliminates damage-induced 5hmC accumulation and elicits chromosome segregation defects in response to replication stress. Our results indicate that the TET enzymes and 5hmC play essential roles in ensuring genome integrity.

INTRODUCTION

Covalent modification of DNA is an essential aspect of genome function. In vertebrates, cytosine methylation catalyzed by DNA methyltransferases is required for proper gene expression throughout development. 5-methylcytosine (5mC) at CpG dinucleotides is normally associated with silencing of genes. The recent discovery that the TET1, TET2, and TET3 dioxygenases actively target 5mC for oxidation into 5-hydroxymethylcytosine (5hmC), 5-formylcytosine (5fC), and 5-carboxylcytosine (5caC) (Ito et al., 2011; Tahiliani et al., 2009) has generated intense interest in active demethylation and its intermediates. Further work has shown that 5hmC is a stable epigenetic modifier of gene expression (Stroud et al., 2011) and that DNA modified with 5hmC generally exhibits an open chromatin configuration (Mendonca et al., 2014). 5hmC is enriched in neural tissue (Hahn et al., 2013; Münzel et al., 2010), where it has been shown to play roles in learning and memory (Rudenko et al., 2013). Recently, a reduction in global 5hmC as a result of decreased TET1 activity, attributed to a loss of ATM, was associated with loss of viability in Purkinje cells, implicating TET activity in the etiology of ataxia-telangiectasia

(Jiang et al., 2015). TET activity and 5hmC levels are known to be high in pluripotent cells (Choi et al., 2014), where it is necessary for successful tissue differentiation (Dawlaty et al., 2014). 5hmC levels are low in cancer cells, which often exhibit misregulated TET activity (Fu et al., 2014; Huang et al., 2013; Ko et al., 2010).

DNA damage is a constant threat to cells that, if left unrepaired, can lead to mutations, genome instability, and disease, especially in the form of cancer. Cells respond to DNA damage by initiating a highly coordinated series of events that culminate with an attempt to repair DNA, referred to as the DNA damage response (DDR) pathway. Increasing evidence suggests that the chromatin environment plays a significant part in the DDR response, specifically the relaxing of chromatin to allow DDR protein complexes access to damaged sites (Ziv et al., 2006).

We have found that covalent modification of DNA also occurs in response to DNA damage. We find a striking localization of 5hmC at large chromosomal regions surrounding endogenous DNA lesions in culture cells (Harrigan et al., 2011; Lukas et al., 2011). We also demonstrate that 5hmC accumulation occurs upon exogenous DNA damage. Lesion-associated 5hmC colocalizes within the same subnuclear domains as induced γH2AX and 53BP1. Finally, we show that the TET enzymes are important for genome integrity, as TET-depleted cells lacking 5hmC suffer from significantly increased chromosome segregation errors in response to replication stress. Our work establishes roles for 5hmC and the TET enzymes in DDR and provides potential explanations for tumorigenicity associated with TET misregulation.

RESULTS

5hmC Localizes to Sites of Endogenous DNA Damage

While characterizing the subnuclear localization of 5hmC in HeLa cells with immunofluorescence, we often observed one or more large (1- to 2-μm diameter) 5hmC foci in a subset of nuclei. These foci were specifically enriched for 5hmC and lacked 5mC (Figure 1A). The frequency and size of these foci recalled the DNA damage-associated and G1-specific 53BP1 nuclear bodies or OPT-domains known from previous observations (Harrigan et al., 2011; Morales et al., 2003; Pombo et al., 1998). To determine whether 5hmC was present in these nuclear bodies, we performed co-immunostaining of 5hmC with 53BP1 or γH2AX
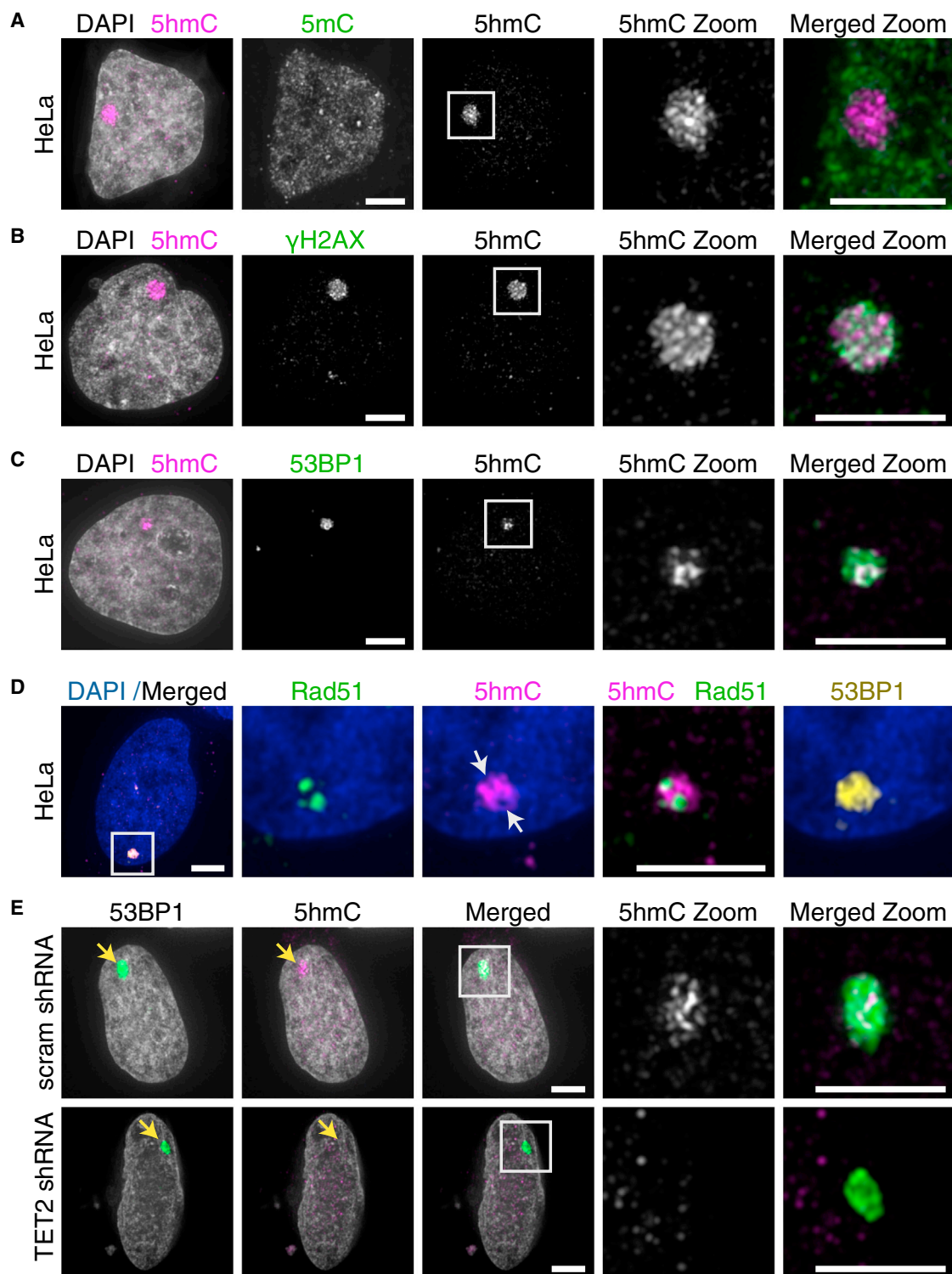
Figure 1. 5hmC Colocalizes with 53BP1 and γH2AX Foci in Unchallenged Human Cell Lines

(A) HeLa cells were stained with DAPI (gray), 5mC (green in merged images), and 5hmC (magenta in merged images).

(B) Colocalization of γH2AX (green in merged images) with 5hmC (magenta in merged images).

(C) Colocalization of 53BP1 (green in merged images) with 5hmC (magenta in merged images).

(legend continued on next page)

and in both cases observed colocalization in common nuclear subdomains (Figures 1B and 1C). Immunostaining of human lung adenocarcinoma cell lines A549 and HCC827 revealed similar colocalization of 53BP1 and 5hmC (Figure S1A). In many cases, the homologous recombination protein RAD51 localized to voids within the 5hmC domains (Figures 1D and S1B), hinting at a functional suborganization of 5hmC foci.

5hmC Localization to DNA Damage in HeLa Cells Depends on TET2

The specific enrichment of 5hmC with DDR proteins suggested a response to DNA damage orchestrated by the TET enzymes, which have been strongly implicated as the sole source of nuclear 5hmC (Ficz et al., 2011). To assess the role of the TET enzymes in creating 5hmC foci, we examined endogenous 53BP1 bodies in the absence of each TET protein. Semiquantitative RT-PCR in HeLa cells showed that TET2 mRNA was approximately 60-fold more abundant than TET1 and 9-fold higher than TET3 (Figure S1C). We then asked whether TET2 was required for the observed 5hmC enrichment by transfecting cells with shRNA targeting TET2. In TET2 knockdown cells, we observed 53BP1 foci that lacked 5hmC staining (Figure 1E). In addition, large 53BP1 foci were rare in TET2 shRNA-treated cells; rather, 53BP1 typically was found as small, dense foci that were also devoid of 5hmC (Figure S1D). Knockdown of TET3 or TET1 did not lead to loss of 5hmC from 53BP1 foci in HeLa cells (Figure S1D).

5hmC Is Locally Enriched by Genotoxic Insults

The robust co-occurrence of 5hmC with γH2AX and 53BP1 suggested that 5hmC is actively enriched in response to endogenous DNA damage. To test this, we examined the effect of genotoxic insults on nuclear 5hmC abundance and distribution. The DNA polymerase inhibitor Aphidicolin (Aph) can reversibly block DNA replication (Ikegami et al., 1978) and causes an increase in the number of 53BP1 nuclear bodies (Lukas et al., 2011). Treatment of HeLa cells with 5 μM Aph led to an increase in 53BP1 foci, which also stained positively for 5hmC (Figure 2A; compare Figure 1C). Numerous small 5hmC foci were seen after 24 hr or 48 hr of continuous Aph treatment. In cells where Aph was washed out following a 24-hr treatment period, we observed very large 53BP1- and 5hmC-positive foci (Figure 2A). By measuring the intensity of 5hmC at 53BP1 sites (Figures 2B, S2A, and S2B), we determined that Aph treatment increased the amount of 53BP1-associated 5hmC beyond the level found at endogenous sites. The intensity of DAPI staining at 5hmC foci also decreased (Figure S2A), indicating a less dense chromatin environment at 5hmC and 53BP1 sites.

To independently confirm that γH2AX-enriched chromatin is also enriched for 5hmC, we measured 5hmC content using chromatin immunoprecipitation (ChIP) with antibodies against γH2AX or canonical histone H2A. Specific β-glycosylation of 5hmC from these pools with ^{3}H-UDP-glucose followed by radiolabel quantitation (Szwagierczak et al., 2010) showed a significant increase in 5hmC content in the γH2AX-containing chromatin fraction over the control H2A fraction, whose 5hmC content was the same as input DNA (Figure 2C). This experiment further shows that 5hmC must be present close to γH2AX sites, since ChIP DNA was digested to a size range of 200 bp to 1 kb. Next, to determine whether DNA breaks increased 5hmC levels globally, we measured 5hmC in HeLa cells treated with Aph. Relative to untreated cells, HeLa cells treated with Aph for 24 hr and then allowed a 24-hr recovery period contained significantly higher levels of genomic 5hmC, whereas HeLa cells treated with Aph continuously for 48 hr were indistinguishable from control cells (Figure 2D). To assess individual cells across the population, we imaged 5hmC and cell-cycle markers in mosaic panel images. Untreated cells or cells treated with Aph for 48 hr had a lower probability of containing 5hmC bodies compared with cells treated for 24 hr and allowed to recover (Figure S2C). Moreover, cells treated with Aph for 48 hr were nearly all Cyclin A2 positive and thus not in the G1 phase of the cell cycle (Figures S2D and S2E), supporting the notion that, as shown previously for 53BP1 nuclear bodies, 5hmC accumulation at DNA damage foci occurs more often in G1.

As 5hmC is the first intermediate in the proposed active DNA demethylation pathway, we investigated whether subsequent intermediates of this pathway, 5fC and 5caC, were also present at 53BP1 sites. We found no 5fC or 5caC at 53BP1 bodies by immunofluorescence (Figure 2E). Combined with the lack of 5mC staining we observed, these results indicate that 5hmC at damaged DNA sites represents a specifically induced, stable epigenetic mark.

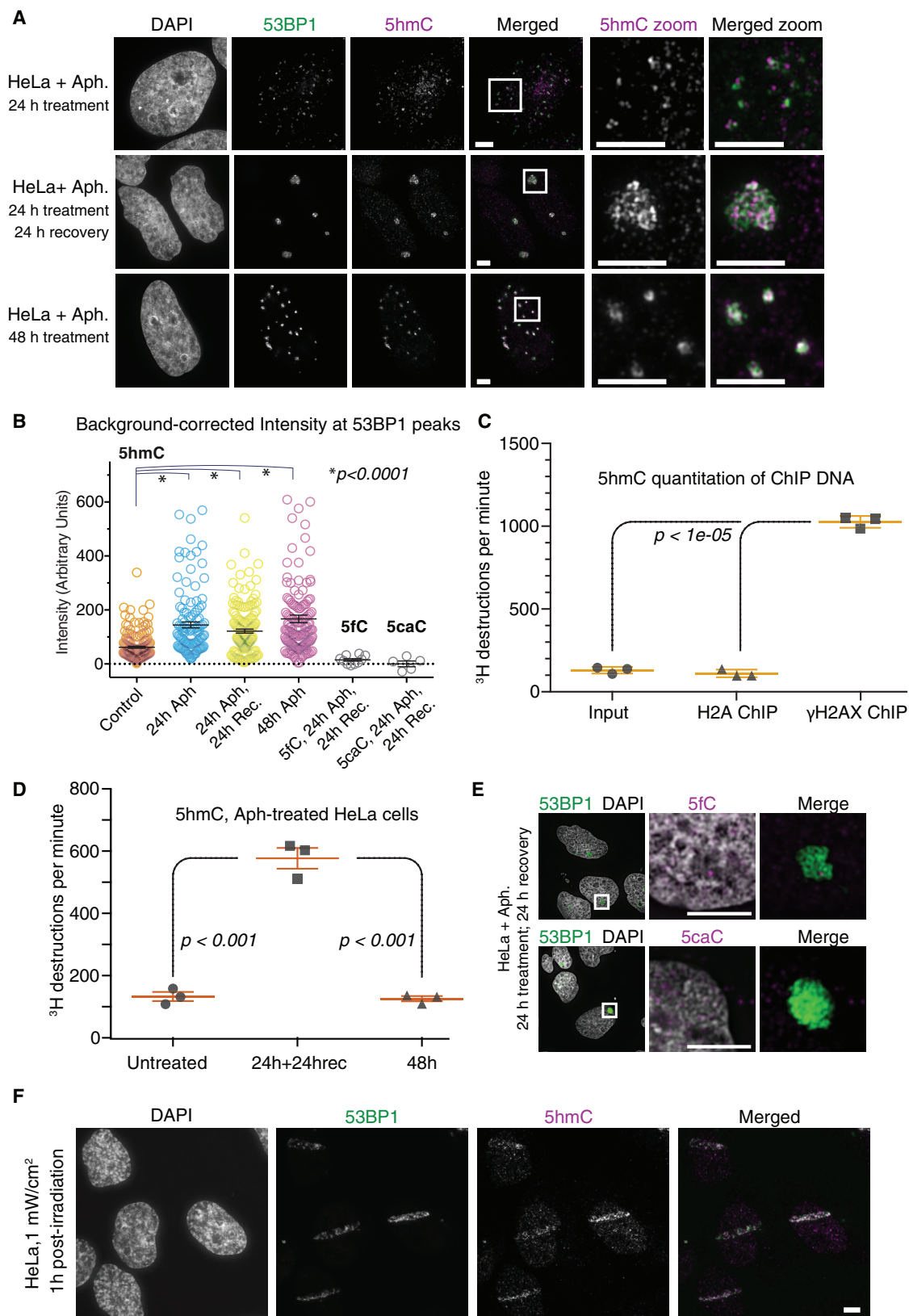## 5hmC Localizes to Microirradiation-Induced DNA Damage

Given that both endogenous and Aph-induced 53BP1 bodies mark DNA lesions caused primarily through replicative stress (Harrigan et al., 2011), we next enquired whether other types of DNA lesions become enriched for 5hmC. We induced DNA double-strand breaks (DSBs) by micro-irradiation with a 405-nm laser on HeLa cells pre-incubated with Hoechst 33342 (Dinant et al., 2007). Irradiation was performed on cells in glass-bottom dishes over 1 hr to establish a time course of DNA damage. In nuclei which had encountered the laser focal point, stripes of 53BP1-co-localized 5hmC were visible within 30 min and were strongest after 1 hr (Figure 2F). Colocalization between γH2AX and 5hmC was also seen in mouse embryonic fibroblasts and C2C12 myoblast cells (G.R.K., unpublished data), indicating that 5hmC is induced at DSBs in both human and mouse cells.

Human Embryonic Stem Cells Show Little Correlation between 5hmC and DNA Damage Markers

Although DNA damage in HeLa cells induces robust colocalization of γH2AX, 53BP1 and 5hmC, cancer-derived cells have been reported to have relatively low levels of 5hmC (Jin et al., 2011). In contrast, pluripotent cells have constitutively high levels of both γH2AX (Banáth et al., 2009) and 5hmC (Ruzov et al., 2011; Tahiliani et al., 2009). To investigate connections between

(D) RAD51 and 5hmC occupy disjoint domains within 53BP1 foci. Shown are DAPI (blue), 53BP1 (yellow), RAD51 (green), and 5hmC (magenta) staining. Arrows indicate voids in 5hmC filled by RAD51 signal.
(E) 5hmC (magenta) in cells treated with control shRNA (top row) or shRNA targeting TET2 (bottom row), compared with 53BP1 (green).
All images are representative of at least three individual experiments. Scale bars represent 5 μm. See also Figure S1.

A

| DAPI | 53BP1 | 5hmC | Merged | 5hmC zoom | Merged zoom |

HeLa + Aph.
24 h treatment

HeLa+ Aph.
24 h treatment
24 h recovery

HeLa + Aph.
48 h treatment

B Background-corrected Intensity at 53BP1 peaks

5hmC

*p<0.0001

Intensity (Arbitrary Units)

5fC   5caC

Control / 24h Aph / 24h Aph, 24h Rec. / 48h Aph / 5fC, 24h Aph, 24h Rec. / 5caC, 24h Aph, 24h Rec.

C 5hmC quantitation of ChIP DNA

³H destructions per minute

p < 1e-05

Input   H2A ChIP   γH2AX ChIP

D 5hmC, Aph-treated HeLa cells

³H destructions per minute

p < 0.001   p < 0.001

Untreated   24h+24hrec   48h

E HeLa + Aph. 24 h treatment; 24 h recovery

| 53BP1 DAPI | 5fC | Merge |
| 53BP1 DAPI | 5caC | Merge |

F HeLa, 1 mW/cm² 1h post-irradiation

| DAPI | 53BP1 | 5hmC | Merged |

(legend on next page)

the high levels of these two marks in pluripotent cells, we next examined the localization of γH2AX and 5hmC in human embryonic stem cells (hESCs). We observed chromatin-wide 5hmC staining throughout the hESC nucleus as previously reported (Takashima et al., 2014), with only a minor subset of γH2AX foci colocalized with 5hmC (Figure 3A).

TET Enzymes Promote Genome Integrity during Replication Stress

Our shRNA-mediated knockdown experiment of TET2 in HeLa cells hinted at a role for the TET-mediated creation of 5hmC in the DDR pathway (Figure 1E). We sought to confirm this observation using mouse embryonic stem cells (mESCs) in which all three TET enzymes had been deleted (TetTKO cells) using CRISPR/ Cas9 genome editing (Figure S3). While Aph treatment of mESCs led to a greater correlation between 5hmC and γH2AX staining (Figure 3B), biochemical quantitation of 5hmC via incorporation of ^{3}H-UDP-glucose to purified DNA revealed that the global levels of 5hmC did not detectably increase upon Aph treatment (Figure S4A) in mESCs. As expected, TetTKO cells had no detectable ^{3}H-UDP-glucose signal. In agreement with this experiment, attempts to immunostain 5hmC in TetTKO mESCs revealed only background staining at levels well below WT mESCs (Figure 3C). This observation demonstrated the specificity of our immunofluorescent detection of 5hmC and ruled out the possibility of 5hmC creation through non-enzymatic means during the experiment. Both WT and TetTKO mESCs were capable of generating γH2AX foci in response to Aph treatment (Figure 3D), which reverted to pre-treatment levels after 24 hr of recovery.

We next sought a sensitive and direct assay to test for persistence of unrepaired DNA damage in the complete absence of TET enzymes and 5hmC. A failure to adequately repair DNA damage sustained during S phase can lead to under-replicated regions that interfere with the separation of chromosomes in mitosis (Naim et al., 2013). We therefore investigated the susceptibility of TetTKO mESC to Aph-induced mitotic defects compared with WT counterparts. We cultured WT and TetTKO mESC under a low dose of Aph (0.2 μM), which has been shown to cause replication stress but still allows most cells to progress through S phase to mitosis (Lukas et al., 2011), and assessed the mitotic competence of cells after 24 hr. Mitotic figures were counted as abnormal if chromosomes or chromosome fragments were found between the main masses of chromatin (Figure 4A). We found that a significantly higher proportion of TetTKO cells displayed such abnormalities, both in Aph-treated (60%) and untreated (17%) conditions, compared to WT cells (28% and 8%, respectively) (Figure 4B). We calculated the partial contributions of loss of the TET enzymes and of 0.2 μM Aph treatment by holding constant the WT and TetTKO base rates of visible errors and by determining what additional error rate induced by Aph treatment would suffice to give the observed total error rate (Figure 4B). This calculation showed that TetTKO cells were more sensitive than WT cells to 0.2 μM Aph, implying that the TET enzymes promote recovery from Aph-induced DNA damage. In line with this finding, dose-response experiments assaying proliferation rates of WT and TetTKO cells under increasing concentrations of Aph showed that TetTKO cells were significantly more sensitive to Aph treatment at levels of 0.1 μM and above (Figure 4C). To investigate whether transcriptional changes due to loss of TET enzymes could be partially responsible for these effects, we examined total RNA from WT and TetTKO cells and found broadly normal expression of DDR pathway genes (Table S3). Moreover, triple-staining experiments showed that γH2AX, 53BP1, and RAD51 colocalized properly in TetTKO cells (Figure S4B). Taken together, these experiments show that the TET enzymes are required to effectively repair Aph-induced DNA damage.

DISCUSSION

Our finding that 5hmC is deposited locally at sites of DNA damage, combined with the results showing that TET enzymes aid in preventing damage-induced chromosome missegregation, strongly suggests an important role for 5hmC in promoting DNA repair and genome integrity. Possible mechanisms for this action could include modification or maintenance of the local chromatin landscape to allow access of other factors, since 5hmC is strongly correlated with an open chromatin conformation (Mellén et al., 2012; Mendonca et al., 2014), whereas 5mC is correlated with repressed chromatin (reviewed in Miranda and Jones, 2007). Consistent with this hypothesis, we observed reduced DAPI intensity, indicative of chromatin decompaction, at 5hmC foci induced in response to DNA damage (Figure S2A). Alternatively, 5hmC could serve as a mark for the recruitment of late-acting repair proteins since we first detect 5hmC at 30-min post-microirradiation, whereas γH2AX and 53BP1 load within the first several minutes after irradiation (Bekker-Jensen et al., 2005; Paull et al., 2000).

Our results demonstrate the necessity of TET2 for production of 5hmC foci at endogenous DNA damage sites in HeLa cells; however, complete characterization of the place and time of action of the different TET proteins is still an open area. Recent reports have established that TET3 drives 5hmC conversion at a time that coincides with the accumulation of γH2AX in two-cell mouse embryos (Nakatani et al., 2015). Another recent report established that TET1 causes global nuclear 5hmC to increase following DNA damage in Purkinje cells (Jiang et al., 2015).

Figure 2. Inducing DNA Damage Results in the Focal Accumulation of 5hmC at Sites of 53BP1

(A) HeLa cells were treated with 5 μM Aphidicolin (Aph) for the indicated times before immunostaining for 53BP1 (green) and 5hmC (magenta).

(B) Background-corrected intensity of 5hmC, 5fC, and 5caC at sites of 53BP1 enrichment is shown for different Aph treatments. Error bars show mean ± SEM. Displayed p values are from two-sample Kolmogorov-Smirnov tests. The number of cells observed was 175 (untreated), 121 (24 hr Aph), 158 (24 hr Aph + 24 hr recovery), 158 (48 hr Aph), 10 (5fC), and 5 (5caC).

(C) Quantification of 5hmC enrichment in DNA isolated by ChIP using the antibodies shown.

(D) Global enrichment of 5hmC in HeLa cells treated with Aph.

(E) 5fC or 5caC staining was performed in HeLa cells exposed to 5 μM Aph for 24 hr followed by 24-hr recovery.

(F) Colocalization of 5hmC (magenta) with 53BP1 (green) on lines induced by laser microirradiation at 405 nm.

All images representative of at least three individual experiments. Scale bars represent 5 μm. See also Figure S2.
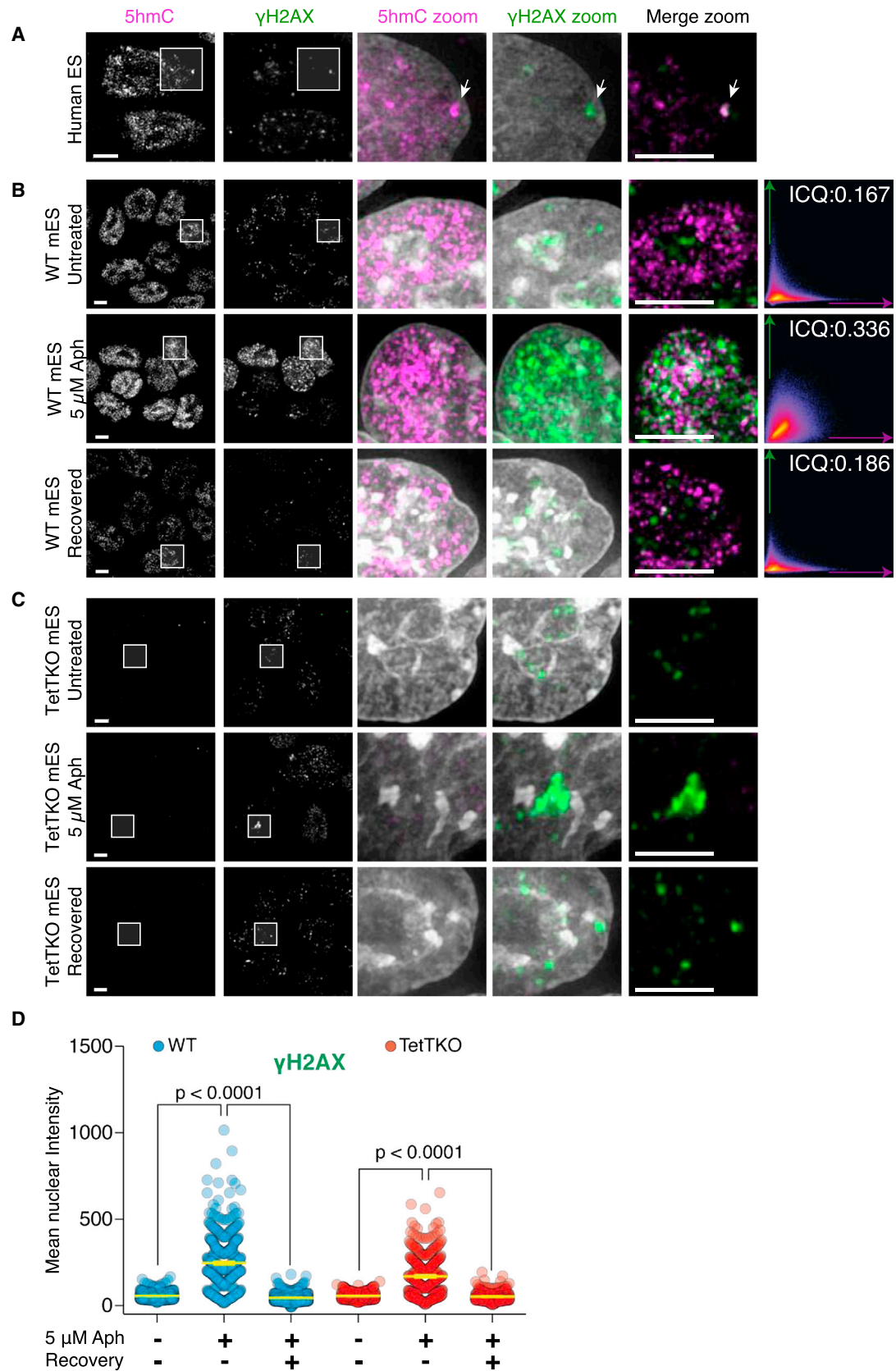
Whether any TET protein is capable of acting downstream of DNA damage or whether specific TETs work in specific cells or stages remains to be determined.

While the accumulation of 5hmC at sites of DNA damage suggests a function of 5hmC or DNA demethylation in promoting repair and thus genome integrity, it is possible that TET enzymes play other roles in DNA repair. For example, increased γH2AX staining observed in TET1-deleted pro-B cells (Cimmino et al., 2015) has been attributed to downregulation of several DNA repair genes. However, our transcriptome analysis of TET triple-knockout mESC showed no significant downregulation of DDR genes, in agreement with a previous analysis (Lu et al., 2014). The sole exception in our dataset is the BRCA2 gene, which shows 2-fold lower mRNA abundance in TetTKO mice. However, since BRCA2 heterozygous mice are WT in tumor susceptibility (Welcsh et al., 2000), it is unlikely that this modest downregulation plays a significant role in the observed phenotype. While gene expression changes could possibly contribute to the defects we observe in TetTKO mESC, the distribution of DNA damage-related proteins such as RAD51 and 53BP1 were comparable to WT in all of our immunostaining experiments. The consistent TET2-dependent localization that we observe of 5hmC with 53BP1, γH2AX, and Rad51 in HeLa and other cancer cell lines suggests a compelling direct role for the TET enzymes in the response to DNA damage.

There may be profound epigenetic consequences concerning both the origin and fate of 5hmC at DNA damage sites. The DNA methyltransferase DNMT1 has been shown to be recruited to sites of induced DNA damage (Mortusewicz et al., 2005) and acts in some capacity to promote genome integrity (Eden et al., 2003; Guo et al., 2004). DNA damage induced by either etoposide in mouse hippocampal neurons or by ionizing radiation in human fibroblast cell lines reportedly caused a global reduction of 5mC (Jiang et al., 2015), whereas others have shown that DNA damage caused by either UV irradiation or doxorubicin in MEFs caused a significant increase of 5mC (Çelik et al., 2015). It is possible that the increased 5hmC we observe derives in part from cytosines that are newly methylated in response to damage and that serve as substrates for TET-mediated 5hmC creation. However, as the large 53BP1-associated domains of 5hmC we observe are never enriched for 5mC, we favor a model in which most of the focal 5hmC we observe derives from preexisting 5mC. Although we attempted to detect site-specific enrichment of 5hmC using TAB-seq (Yu et al., 2012a, 2012b), targeting three regions (see Supplemental Experimental Procedures) previously shown to be enriched for DSBs in HeLa cells treated with Aph (Crosetto et al., 2013), no enrichment of 5hmC was detected (G.R.K., X.L., and P.M.C., unpublished data). This negative result could be explained by a low probability of breaks occurring at a specified site and would also be consistent with a requirement for pre-existing 5mC, which was absent at the sites we examined, for producing damage-associated 5hmC. Future studies employing genome-wide detection of 5hmC at very high sequencing depth, combined with traditional bisulfite sequencing to reveal the 5mC distribution, will therefore be required to map the distribution of damage-induced 5hmC at the nucleotide level. Further, since we never observed large 5hmC foci without 53BP1 staining, we conclude that the bulk of this damage-induced 5hmC is removed along with 53BP1 during S phase (Lukas et al., 2011). Failure to return newly 5hmC-marked regions to their previous methylation status could result in long-term changes in gene expression in response to DNA damage. Finally, our results imply that loss of TET enzymes and 5hmC depletion could contribute significantly to genome instability and inaccurate chromosome segregation, perhaps explaining the correlation of low 5hmC levels with cancer (Tan and Shi, 2012). The damage-modulated focal enrichment of the covalent DNA modification 5hmC by the TET enzymes implies far-reaching roles for epigenetics in regulating genome integrity.

EXPERIMENTAL PROCEDURES

Cell Culture

HeLa, HCC827, A549, C2C12, and MEF cells were grown in DMEM with 10% fetal bovine serum (FBS). All mESCs (male C57BL/6J) were grown under LIF+2i conditions (Ying et al., 2008). hESCs (H1 line) were grown in ReproCell Primate media supplemented with FGF2 on inactivated MEFs. ES-grade matrigel (Fisher Scientific, Catalog # 354277) was used to grow mESCs and hESCs on glass surfaces in the absence of MEFs. Cells were treated with Aphidicolin (Sigma-Aldrich) dissolved in DMSO. All transfections were performed with Lipofectamine 2000 (Life Technologies). In HeLa cells, TET knockdown was performed with HuSH shRNA 29-mer plasmids (Origene). Mammalian codon-optimized Cas9, and gRNAs targeting the TET1, TET2, and TET3 genes were used to generate TetTKO mESC as described elsewhere (Horii et al., 2013). TET enzyme deletions were confirmed by PCR-RFLP analysis and sequencing (Figure S3).

Chromatin Immunoprecipitation

Native chromatin isolation (for detailed description, see the Supplemental Experimental Procedures) was performed using 50×10^6 HeLa cells per sample. In brief, isolated chromatin was resuspended at 0.5 mg/ml before micrococcal nuclease digestion (NEB, M0247S) as per manufacturer's specifications. Dynabeads Protein G (Thermo Scientific) were incubated with 30 μg ChIP grade antibody (H2A, Abcam, ab177308 or γH2AX, Millipore, 05-636) before the addition of 100–200 μg of cleared chromatin. Bead-chromatin mixture was incubated overnight at 4°C before magnetic separation of bound chromatin as per the manufacturer's directions.

Quantification of Global 5hmC

Isolated DNA (125 ng per sample) was labeled in a reaction with 50 mM ^{3}H-UDP-glucose (Perkin Elmer) and 10 mM β-glucosyltransferase before measurement by scintillation counting as described (Otani et al., 2013) with some modifications (see the Supplemental Experimental Procedures).

Figure 3. TET-1,-2,-3 Triple-Knockout mESC Lack 5hmC but Increase γH2AX in Response to Aphidicolin Treatment
(A) hESC immunostained for 5hmC (magenta) and γH2AX (green). Arrows indicate colocalization.
(B and C) WT (B) and TET triple knockout (TetTKO) (C) mESCs untreated or treated with 5 μM Aphidicolin (Aph) for 1 hr or allowed to recover for 24 hr before fixation. Intensity correlation quotients (ICQ) show staining dependency (colocalization) as values between 0 and 0.5, where 0.5 is complete colocalization and 0 is no colocalization.
(D) Corrected total nuclear fluorescence of γH2AX measured in WT and TetTKO mESC under different Aph regimes. For WT, the number of cells observed was 504 (untreated), 380 (24 hr Aph), 455 (24 hr Aph + 24 hr recovery); for TetTKO, numbers were 393 (untreated), 345 (24h Aph), 327 (24h Aph + 24h recovery).
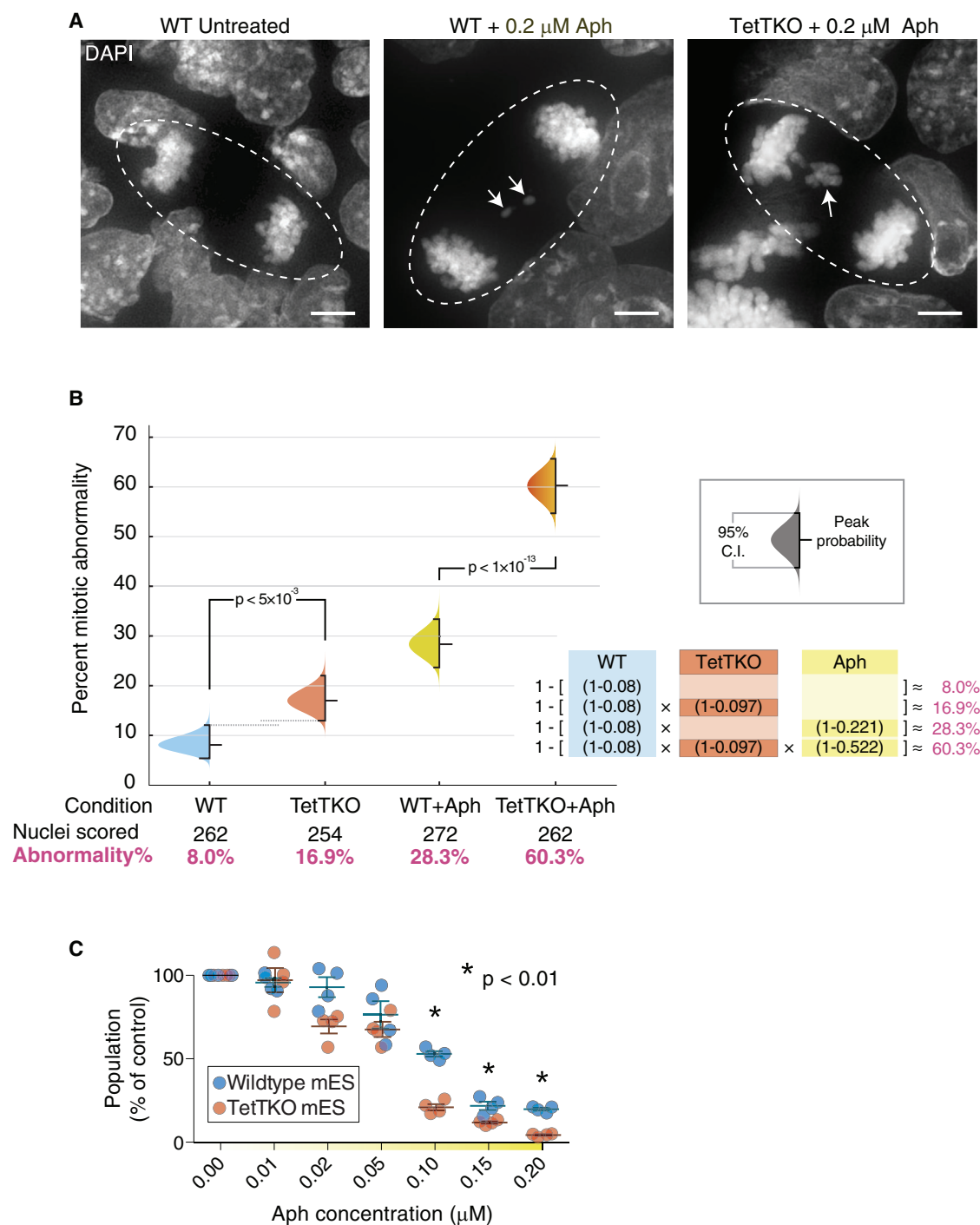See also Figure S3.

Figure 4. Mitotic Characterization of WT and TetTKO mESCs

(A) DAPI-stained representative examples of mitotic figures: normal mitosis in WT untreated (left) and mitotic abnormalities (arrows) in WT (middle) and TetTKO (right) mESC treated with 0.2 μM Aph for 24 hr. Scale bar represents 5 μm.

(B) Top: the frequency of observed mitotic abnormalities in anaphase and telophase nuclei (two independent experiments). Calculated probability distributions are shown centered on the actual observed fraction of mitotic errors, with 95% CI in brackets. Right: the partial contribution of Aph to the observed frequency of mitotic abnormalities in WT or TetTKO cells. Columns show the effect of each condition, which are multiplied across the rows to produce the observed mitotic abnormality rate.

(C) Proliferation rates of WT and TetTKO after 3 days of culture with the indicated concentrations of Aph. Error bars show mean ± SEM. Displayed p values are from one-way ANOVA using a Bonferroni post test to compare WT rates to TetTKO rates under each Aph concentration.

See also Figure S4 and Tables S1, S2, and S3.

Microirradiation

Cells were microirradiated on a modified Nikon Ti Eclipse microscope (see the Supplemental Experimental Procedures) after pre-incubation with Hoechst 33342 dye at 1 μg/ml for 1 hr.

Immunofluorescence Microscopy and Analysis

PFA-fixed cells were washed and permeabilized before blocking and overnight incubation with primary antisera. Visualization of 5mC, 5hmC, 5fC, and 5caC was performed with extended permeabilization and 2N HCl treatment (Çelik et al., 2014; Takashima et al., 2014). Cells were washed and incubated with secondary antisera, stained with DAPI, and mounted in glycerol containing 4% w/v n-propyl gallate. GFP-Booster (Chromotek, Catalog #GBA-488) was used to enhance GFP signal where necessary. Cells were imaged on a widefield DeltaVision deconvolution system (Applied Precision/GE Healthcare; see the Supplemental Experimental Procedures). For mitotic aberration counts, anaphase and telophase cells were imaged randomly by recording 3D images of all anaphase and telophase cells encountered during a large area scan, and scored blindly by two people.

Semiquantitative Real-Time PCR

Total RNA was extracted using RNeasy mini kit (QIAGEN) and DNase treated before reverse transcription with random hexamers (SuperScript III, Invitrogen). RT-PCR was performed with SYBR Green reagents using the StepOnePlus Real-Time PCR System (Applied Biosystems). Relative expression was calculated using β-actin as an endogenous reference gene (see the Supplemental Experimental Procedures).

ACCESSION NUMBERS

The transcriptome microarray dataset discussed in this article has been deposited in NCBI GEO and is available under accession number GEO: GSE72998.

SUPPLEMENTAL INFORMATION

Supplemental Information includes Supplemental Experimental Procedures, four figures, and three tables and can be found with this article online at http://dx.doi.org/10.1016/j.celrep.2016.01.035.

AUTHOR CONTRIBUTIONS

G.R.K., I.S., S.T., I.H., and P.M.C. designed experiments. G.R.K., X.L., I.S., T.H., and P.M.C. performed experiments, and G.R.K. and P.M.C. analyzed data and wrote the paper.

REFERENCES

Banáth, J.P., Bañuelos, C.A., Klokov, D., MacPhail, S.M., Lansdorp, P.M., and Olive, P.L. (2009). Explanation for excessive DNA single-strand breaks and endogenous repair foci in pluripotent mouse embryonic stem cells. Exp. Cell Res. 315, 1505–1520.

Bekker-Jensen, S., Lukas, C., Melander, F., Bartek, J., and Lukas, J. (2005). Dynamic assembly and sustained retention of 53BP1 at the sites of DNA damage are controlled by Mdc1/NFBD1. J. Cell Biol. 170, 201–211.

Çelik, S., Li, Y., and O'Neill, C. (2014). The exit of mouse embryonic fibroblasts from the cell-cycle changes the nature of solvent exposure of the 5′-methylcytosine epitope within chromatin. PLoS ONE 9, e92523.

Çelik, S., Li, Y., and O'Neill, C. (2015). The effect of DNA damage on the pattern of immune-detectable DNA methylation in mouse embryonic fibroblasts. Exp. Cell Res. 339, 20–34.

Choi, I., Kim, R., Lim, H.W., Kaestner, K.H., and Won, K.J. (2014). 5-hydroxymethylcytosine represses the activity of enhancers in embryonic stem cells: a new epigenetic signature for gene regulation. BMC Genomics 15, 670.

Cimmino, L., Dawlaty, M.M., Ndiaye-Lobry, D., Yap, Y.S., Bakogianni, S., Yu, Y., Bhattacharyya, S., Shaknovich, R., Geng, H., Lobry, C., et al. (2015). TET1 is a tumor suppressor of hematopoietic malignancy. Nat. Immunol. 16, 653–662.

Crosetto, N., Mitra, A., Silva, M.J., Bienko, M., Dojer, N., Wang, Q., Karaca, E., Chiarle, R., Skrzypczak, M., Ginalski, K., et al. (2013). Nucleotide-resolution DNA double-strand break mapping by next-generation sequencing. Nat. Methods 10, 361–365.

Dawlaty, M.M., Breiling, A., Le, T., Barrasa, M.I., Raddatz, G., Gao, Q., Powell, B.E., Cheng, A.W., Faull, K.F., Lyko, F., and Jaenisch, R. (2014). Loss of Tet enzymes compromises proper differentiation of embryonic stem cells. Dev. Cell 29, 102–111.

Dinant, C., de Jager, M., Essers, J., van Cappellen, W.A., Kanaar, R., Houtsmuller, A.B., and Vermeulen, W. (2007). Activation of multiple DNA repair pathways by sub-nuclear damage induction methods. J. Cell Sci. 120, 2731–2740.

Eden, A., Gaudet, F., Waghmare, A., and Jaenisch, R. (2003). Chromosomal instability and tumors promoted by DNA hypomethylation. Science 300, 455.

Ficz, G., Branco, M.R., Seisenberger, S., Santos, F., Krueger, F., Hore, T.A., Marques, C.J., Andrews, S., and Reik, W. (2011). Dynamic regulation of 5-hydroxymethylcytosine in mouse ES cells and during differentiation. Nature 473, 398–402.

Fu, H.-L., Ma, Y., Lu, L.-G., Hou, P., Li, B.-J., Jin, W.-L., and Cui, D.-X. (2014). TET1 exerts its tumor suppressor function by interacting with p53-EZH2 pathway in gastric cancer. J. Biomed. Nanotechnol. 10, 1217–1230.

Guo, G., Wang, W., and Bradley, A. (2004). Mismatch repair genes identified using genetic screens in Blm-deficient embryonic stem cells. Nature 429, 891–895.

Hahn, M.A., Qiu, R., Wu, X., Li, A.X., Zhang, H., Wang, J., Jui, J., Jin, S.-G., Jiang, Y., Pfeifer, G.P., and Lu, Q. (2013). Dynamics of 5-hydroxymethylcytosine and chromatin marks in Mammalian neurogenesis. Cell Rep. 3, 291–300.

Harrigan, J.A., Belotserkovskaya, R., Coates, J., Dimitrova, D.S., Polo, S.E., Bradshaw, C.R., Fraser, P., and Jackson, S.P. (2011). Replication stress induces 53BP1-containing OPT domains in G1 cells. J. Cell Biol. 193, 97–108.

Horii, T., Morita, S., Kimura, M., Kobayashi, R., Tamura, D., Takahashi, R.-U., Kimura, H., Suetake, I., Ohata, H., Okamoto, K., et al. (2013). Genome engineering of mammalian haploid embryonic stem cells using the Cas9/RNA system. PeerJ 1, e230.

Huang, H., Jiang, X., Li, Z., Li, Y., Song, C.-X., He, C., Sun, M., Chen, P., Gurbuxani, S., Wang, J., et al. (2013). TET1 plays an essential oncogenic role in MLL-rearranged leukemia. Proc. Natl. Acad. Sci. USA 110, 11994–11999.

Ikegami, S., Taguchi, T., Ohashi, M., Oguro, M., Nagano, H., and Mano, Y. (1978). Aphidicolin prevents mitotic cell division by interfering with the activity of DNA polymerase-α. Nature 275, 458–460.

Ito, S., Shen, L., Dai, Q., Wu, S.C., Collins, L.B., Swenberg, J.A., He, C., and Zhang, Y. (2011). Tet proteins can convert 5-methylcytosine to 5-formylcytosine and 5-carboxylcytosine. Science *333*, 1300–1303.

Jiang, D., Zhang, Y., Hart, R.P., Chen, J., Herrup, K., and Li, J. (2015). Alteration in 5-hydroxymethylcytosine-mediated epigenetic regulation leads to Purkinje cell vulnerability in ATM deficiency. Brain *138*, 3520–3536.

Jin, S.-G., Jiang, Y., Qiu, R., Rauch, T.A., Wang, Y., Schackert, G., Krex, D., Lu, Q., and Pfeifer, G.P. (2011). 5-Hydroxymethylcytosine is strongly depleted in human cancers but its levels do not correlate with IDH1 mutations. Cancer Res. *71*, 7360–7365.

Ko, M., Huang, Y., Jankowska, A.M., Pape, U.J., Tahiliani, M., Bandukwala, H.S., An, J., Lamperti, E.D., Koh, K.P., Ganetzky, R., et al. (2010). Impaired hydroxylation of 5-methylcytosine in myeloid cancers with mutant TET2. Nature *468*, 839–843.

Lu, F., Liu, Y., Jiang, L., Yamaguchi, S., and Zhang, Y. (2014). Role of Tet proteins in enhancer activity and telomere elongation. Genes Dev. *28*, 2103–2119.

Lukas, C., Savic, V., Bekker-Jensen, S., Doil, C., Neumann, B., Pedersen, R.S., Grøfte, M., Chan, K.L., Hickson, I.D., Bartek, J., and Lukas, J. (2011). 53BP1 nuclear bodies form around DNA lesions generated by mitotic transmission of chromosomes under replication stress. Nat. Cell Biol. *13*, 243–253.

Mellén, M., Ayata, P., Dewell, S., Kriaucionis, S., and Heintz, N. (2012). MeCP2 binds to 5hmC enriched within active genes and accessible chromatin in the nervous system. Cell *151*, 1417–1430.

Mendonca, A., Chang, E.H., Liu, W., and Yuan, C. (2014). Hydroxymethylation of DNA influences nucleosomal conformation and stability in vitro. Biochim. Biophys. Acta *1839*, 1323–1329.

Miranda, T.B., and Jones, P.A. (2007). DNA methylation: the nuts and bolts of repression. J. Cell. Physiol. *213*, 384–390.

Morales, J.C., Xia, Z., Lu, T., Aldrich, M.B., Wang, B., Rosales, C., Kellems, R.E., Hittelman, W.N., Elledge, S.J., and Carpenter, P.B. (2003). Role for the BRCA1 C-terminal repeats (BRCT) protein 53BP1 in maintaining genomic stability. J. Biol. Chem. *278*, 14971–14977.

Mortusewicz, O., Schermelleh, L., Walter, J., Cardoso, M.C., and Leonhardt, H. (2005). Recruitment of DNA methyltransferase I to DNA repair sites. Proc. Natl. Acad. Sci. USA *102*, 8905–8909.

Münzel, M., Globisch, D., Brückl, T., Wagner, M., Welzmiller, V., Michalakis, S., Müller, M., Biel, M., and Carell, T. (2010). Quantification of the sixth DNA base hydroxymethylcytosine in the brain. Angew. Chem. Int. Ed. Engl. *49*, 5375–5377.

Naim, V., Wilhelm, T., Debatisse, M., and Rosselli, F. (2013). ERCC1 and MUS81-EME1 promote sister chromatid separation by processing late replication intermediates at common fragile sites during mitosis. Nat. Cell Biol. *15*, 1008–1015.

Nakatani, T., Yamagata, K., Kimura, T., Oda, M., Nakashima, H., Hori, M., Sekita, Y., Arakawa, T., Nakamura, T., and Nakano, T. (2015). Stella preserves maternal chromosome integrity by inhibiting 5hmC-induced γH2AX accumulation. EMBO Rep. *16*, 582–589.

Otani, J., Kimura, H., Sharif, J., Endo, T.A., Mishima, Y., Kawakami, T., Koseki, H., Shirakawa, M., Suetake, I., and Tajima, S. (2013). Cell cycle-dependent turnover of 5-hydroxymethyl cytosine in mouse embryonic stem cells. PLoS ONE *8*, e82961.

Paull, T.T., Rogakou, E.P., Yamazaki, V., Kirchgessner, C.U., Gellert, M., and Bonner, W.M. (2000). A critical role for histone H2AX in recruitment of repair factors to nuclear foci after DNA damage. Curr. Biol. *10*, 886–895.

Pombo, A., Cuello, P., Schul, W., Yoon, J.B., Roeder, R.G., Cook, P.R., and Murphy, S. (1998). Regional and temporal specialization in the nucleus: a transcriptionally-active nuclear domain rich in PTF, Oct1 and PIKA antigens associates with specific chromosomes early in the cell cycle. EMBO J. *17*, 1768–1778.

Rudenko, A., Dawlaty, M.M., Seo, J., Cheng, A.W., Meng, J., Le, T., Faull, K.F., Jaenisch, R., and Tsai, L.-H. (2013). Tet1 is critical for neuronal activity-regulated gene expression and memory extinction. Neuron *79*, 1109–1122.

Ruzov, A., Tsenkina, Y., Serio, A., Dudnakova, T., Fletcher, J., Bai, Y., Chebotareva, T., Pells, S., Hannoun, Z., Sullivan, G., et al. (2011). Lineage-specific distribution of high levels of genomic 5-hydroxymethylcytosine in mammalian development. Cell Res. *21*, 1332–1342.

Stroud, H., Feng, S., Morey Kinney, S., Pradhan, S., and Jacobsen, S.E. (2011). 5-Hydroxymethylcytosine is associated with enhancers and gene bodies in human embryonic stem cells. Genome Biol. *12*, R54.

Szwagierczak, A., Bultmann, S., Schmidt, C.S., Spada, F., and Leonhardt, H. (2010). Sensitive enzymatic quantification of 5-hydroxymethylcytosine in genomic DNA. Nucleic Acids Res. *38*, e181.

Tahiliani, M., Koh, K.P., Shen, Y., Pastor, W.A., Bandukwala, H., Brudno, Y., Agarwal, S., Iyer, L.M., Liu, D.R., Aravind, L., and Rao, A. (2009). Conversion of 5-methylcytosine to 5-hydroxymethylcytosine in mammalian DNA by MLL partner TET1. Science *324*, 930–935.

Takashima, Y., Guo, G., Loos, R., Nichols, J., Ficz, G., Krueger, F., Oxley, D., Santos, F., Clarke, J., Mansfield, W., et al. (2014). Resetting transcription factor control circuitry toward ground-state pluripotency in human. Cell *158*, 1254–1269.

Tan, L., and Shi, Y.G. (2012). Tet family proteins and 5-hydroxymethylcytosine in development and disease. Development *139*, 1895–1902.

Welcsh, P.L., Owens, K.N., and King, M.-C. (2000). Insights into the functions of BRCA1 and BRCA2. Trends Genet. *16*, 69–74.

Ying, Q.-L., Wray, J., Nichols, J., Batlle-Morera, L., Doble, B., Woodgett, J., Cohen, P., and Smith, A. (2008). The ground state of embryonic stem cell self-renewal. Nature *453*, 519–523.

Yu, M., Hon, G.C., Szulwach, K.E., Song, C.-X., Jin, P., Ren, B., and He, C. (2012a). Tet-assisted bisulfite sequencing of 5-hydroxymethylcytosine. Nat. Protoc. *7*, 2159–2170.

Yu, M., Hon, G.C., Szulwach, K.E., Song, C.-X., Zhang, L., Kim, A., Li, X., Dai, Q., Shen, Y., Park, B., et al. (2012b). Base-resolution analysis of 5-hydroxymethylcytosine in the mammalian genome. Cell *149*, 1368–1380.

Ziv, Y., Bielopolski, D., Galanty, Y., Lukas, C., Taya, Y., Schultz, D.C., Lukas, J., Bekker-Jensen, S., Bartek, J., and Shiloh, Y. (2006). Chromatin relaxation in response to DNA double-strand breaks is modulated by a novel ATM- and KAP-1 dependent pathway. Nat. Cell Biol. *8*, 870–876.